Allergologia et immunopathologia
Sociedad Española de Inmunología Clínica, Alergología y Asma Pediátrica
www.all-imm.com

ORIGINAL ARTICLE

OPEN ACCESS

# From bioinformatics to anti-inflammation and immune regulation: ACT001 in lipopolysaccharide-induced lung injury

**Yan Fan[a†], Yuanlin Wang[b†], Weiwei Zhang[c], Keliang Xie[a,b*]**

[a]*Department of Critical Care Medicine, Tianjin Medical University General Hospital, Tianjin, China*
[b]*Department of Anesthesiology, Tianjin Institute of Anesthesiology, Tianjin Medical University General Hospital, Tianjin, China*
[c]*School of Medicine, NanKai University, Tianjin, China*

[†]Yan Fan and Yuanlin Wang contributed equally to this work

Received 6 June 2024; Accepted 1 August 2024
Available online 1 November 2024

**KEYWORDS**
ACT001;
acute lung injury;
NLRP3;
pyroptosis;
single and spatial transcriptomics

**Abstract**
*Background*: ACT001 is a potent anti-inflammatory small-molecule drug. However, the single cell and spatial molecular basis of pyroptosis and whether ACT001 exerts a therapeutic effect by preventing pyroptosis on acute lung injury (ALI) remains unclear.
*Methods*: The bioinformatics approach was employed to identify single cell and spatial landscape of nucleotide-binding domains and leucine-rich repeat protein 3 (NLRP3)-dependent pyroptosis in lipopolysaccharide (LPS) and influenza virus-induced ALI. Molecular docking was performed to elucidate the relationship between ACT001 and NLRP3. LPS-induced ALI mice model was established. Histopathological analysis and bronchoalveolar lavage fluid collection were conducted to investigate the anti-inflammatory and protective effects. In vitro experiments were also performed on bone marrow-derived macrophages to explore the effect of ACT001 on the balance of mitochondrial fusion and fission protein.
*Results*: Single cell transcriptomic and spatial transcriptomic analysis predicted that NLRP3-dependent pyroptosis significantly correlated with the development of ALI both in single cell and spatial distribution. Molecular docking provided a stable and reliable docking between ACT001 and NLRP3. ACT001 improved the 7-day survival of mice by approximately 50% over the loading dose of LPS-induced ALI. ACT001 (5 uM) attenuated the disruption of mitochondrial integrity and reactive oxygen species. Further, ACT001 reduced the overexpression of the mitochondrial fission protein DRP1 without affecting fusion protein Mitofusin2 levels. Moreover, ACT001 exerted a similar protective effect of suppressing pyroptosis as the DRP1-inhibitor Mdivi-1.
*Conclusions*: Our study revealed that pyroptosis genes were highly expressed in single-cell and spatial mapping along the first week of ALI occurrence. ACT001 attenuates ALI by reducing the NLRP3-dependent pyroptosis and balancing mitochondrial fission and fusion.


[*]**Corresponding author:** Ke-liang Xie, Department of Anesthesiology and Critical Care Medicine, Tianjin Institute of Anesthesiology, Tianjin Medical University General Hospital, No. 154, Anshan Road, Heping District, Tianjin, China. *Email address*: mazuixkl@163.com

https://doi.org/10.15586/aei.v52i6.1146

## Introduction

Acute lung injury (ALI) is the first cause of sepsis-related death.[1] Lipopolysaccharides (LPS) from bacteria are the primary cause of induction of infective ALI in live and clinical environments. Conventional drugs often have side effects, thereby limiting their clinical use.[2] However, herbs extracted from traditional Chinese medicine plants are speculated to address these disadvantages. Besides, advances in precise medicine have provided more possibilities for Chinese medicine.[3]

Pyroptosis is a critical natural immune response in the body, which mediates protection against infection. However, over-activation of pyroptosis might result in inflammation-related diseases, including septic shock,[4] systemic inflammatory response syndrome (SIRS),[5] or increased risk of secondary infection. Therefore, identifying small molecule inhibitors targeting the inflammasome is an important research focus for developing effective treatment against inflammation in the future. Nucleotide-binding domains and leucine-rich repeat protein 3 (NLRP3) inflammasome are activated in response to tissue injury and regulate the processing of inflammation-associated proteins, including gasdermin D (GSDMD) and interleukin (IL)-1β.[6] Recent studies have shown that inactivated NLRP3 is bound together by leucine-rich repeat sequence interactions to form a bicyclic cage that protects PYD and prevents premature activation.[7] Moreover, mitochondrial reactive oxygen species and oxidized DNA fragments activate NLRP3 inflammasome.[8] However, the precise pathways causing NLRP3 inflammasome assembly and activation after cell injury remain elusive. Importantly, persistent NLRP3 signaling is strongly linked to inflammation-related disorders, including septic shock, SIRS, atherosclerosis, and inflammatory bowel diseases.[9] Therefore, there is an urgent need to clarify the mechanism of NLRP3 inflammasome activation to provide therapeutic tools for treating diseases including ALI.

Recent advances in bioinformatics have made possible the investigation of gene expression changes in multiple levels, including single-cell and spatial tissues.[10,11] Previous analysis of single-cell transcriptomics primarily focuses on the immune cells or endothelial cell subtypes changes of lungs with sepsis.[12,13] Spatial studies based on transcriptomics expand the understanding of the relationship between mRNA and disease status or entire pathogenically physical function.[14]

ACT001 is a natural product parthenolide (PTL) extracted from *Magnolia officinalis* with antitumor, anti-inflammatory, and antioxidant activities.[15,16] ACT001 is believed to have pharmacological activities, with better aqueous solubility and stability, compared to PTL, and has a wide range of potential clinical applications.[17-19] It has been shown that ACT001 is a potential drug designated by the FDA as an orphan drug for glioblastoma treatment. The drug is being evaluated in several clinical trials (ACTRN12616000228482, Australia New Zealand Clinical Trials Registry; China Clinical Trials Registration (ChiCTR-OIC-17013604).[20] Additionally, a recent study concluded that parthenolide is one of the promising herbal candidates for the clinical treatment of COVID-19.[21] However, whether ACT001 benefits the host by modulating NLRP3 inflammasome remains unclear.

This work sought to investigate the protective effects of ACT001 in LPS-related ALI and its possible mechanisms. We performed bioinformatics analysis, molecular docking, and in vivo and in vitro experiments to provide novel insights on pyroptosis and ACT001 in LPS-related ALI. The mice model was constructed by endotracheal dripping LPS (10 mg/kg) to induce ALI.

## Methods

Figure 1 shows the procedure for the whole study.

### *Mice and treatment*

Six- to eight-weeks-old specific pathogen-free (SPF) C57BL/6J male mice were purchased from The Laboratory Animal Center of the Chinese Academy of Medical Sciences in Beijing, China. All animal experiments were performed under the Institutional Research Ethics Committee of the Animal Ethics Committee of the Tianjin Medical University General Hospital with approval number [IRB2022-DWFL-587]. Mice were housed under a regular 12-h light/dark cycle and acclimated to laboratory conditions for 1 week before testing at a constant temperature. Mice were anesthetized with 2.5% 2,2,2-tribromoethanol (MedChemExpress, USA) via intraperitoneal injection to eliminate pain for any incisive operations. The mice were randomly divided into four groups (5 mice per group) as follows: (a) PBS + PBS, (b) LPS + PBS, (c) LPS + ACT001 (100 mg/kg), and (d) LPS + ACT001 (200 mg/kg). Under anesthesia, the tongue was pulled outward using curved forceps, and 200 μL gel loading tips were introduced into the trachea. Note that the angiocatheter should be parallel to the tracheal plane. ACT001 (100 mg/kg or 200 mg/kg in 50 μL PBS) was carefully loaded into the tips or a similar volume of PBS was injected into the trachea 2 h before the LPS challenge (10 mg/kg, Sigma, USA). Bronchoalveolar lavage fluid (BALF) and lung tissues were collected for analysis 24 h after the LPS challenge. Survival and body weights were recorded daily before and during the experiment for 7 days.

### *Hub genes among nucleotide-binding oligomerization domain (NOD) pathway and pyroptosis*

Nucleotide-binding oligomerization domain (NOD)-like receptor pathway-related genes were downloaded from the GSEA (Gene Set Enrichment Analysis) database (https://www.gsea-msigdb.org/). According to Gadepalli et al.,[22] we obtained a pyroptosis gene set from the XDeathDB online website using a cell death-related search engine. Then, an online Venn diagram website tool, Evenn,[23] was used to search common genes between NOD-like receptors and pyroptosis. Further, a protein–protein interaction (PPI) network was constructed by importing common genes into a string database.[24] Genes of the highest degree, which played the most important role in the entire network, were

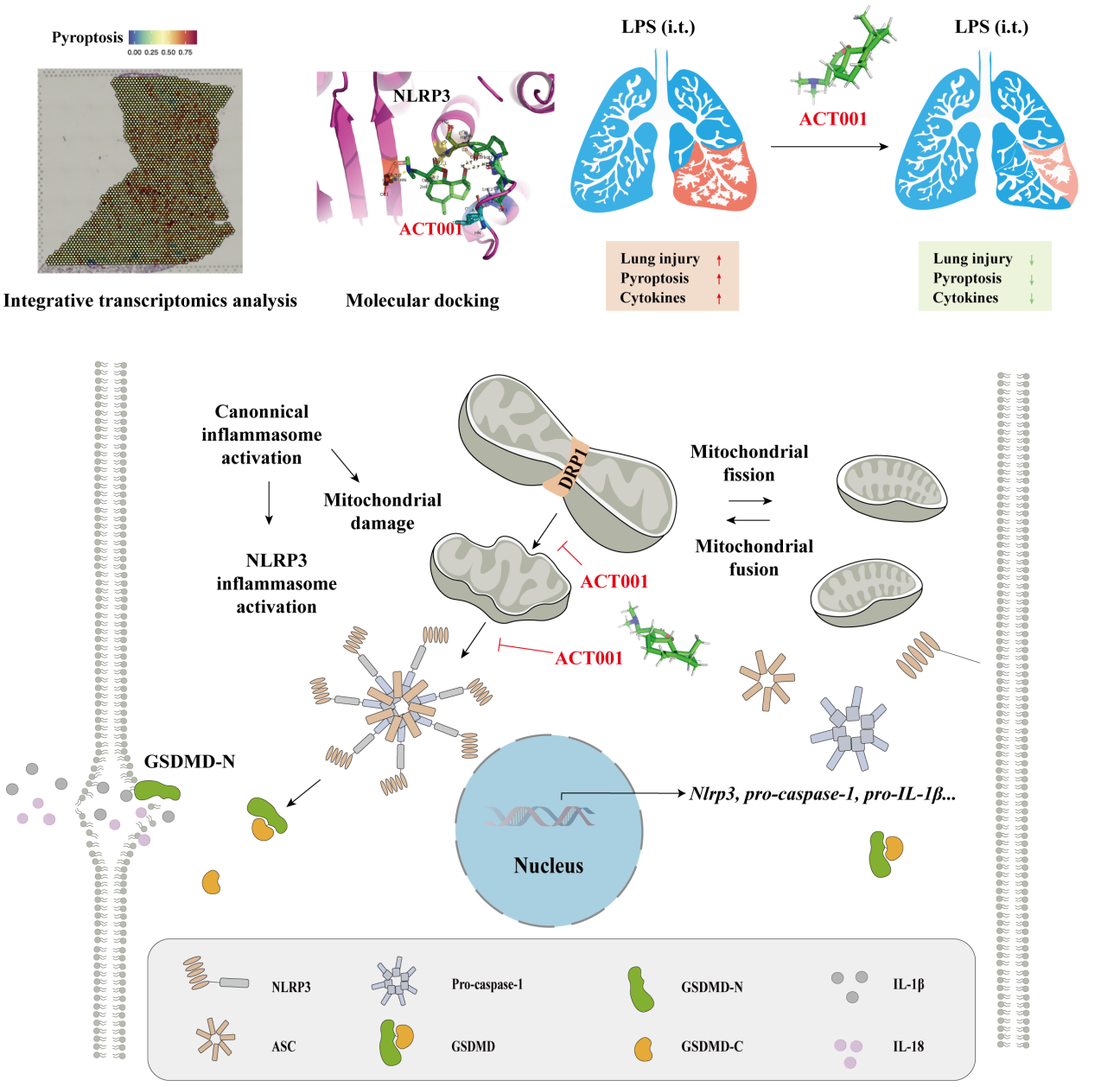


**Figure 1** Schematic of ACT001 inhibition of NLRP3 inflammasome activation to attenuate acute lung injury (ALI). Integrative transcriptomic analysis revealed a strong correlation between NLRP3-associated pyroptosis and ALI. Molecular docking showed that ACT001 and NLRP3 could be stably docked. In vivo and in vitro experiments confirmed that ACT001 attenuated ALI caused by NLRP3-associated pyroptosis. Mechanistically, ACT001 directly inhibits NLRP3 proteins and the expression of the mitochondrial fission protein DRP1 to attenuate NLRP3-dependent pyroptosis.

screened and specially analyzed in subsequent single-cell transcriptome analysis.

### *Data acquisition and preprocessing*

Single-cell transcriptome matrixes were downloaded from the GEO database. Lung endothelial cell datasets including wild type and LPS treating type, GSE148499,[25] comprised five timepoint groups (6 h; and 1, 2, 3, and 7 days) after LPS exposure. We also downloaded GSE218884, a lung resident macrophage dataset. Two phenotypes, homeostasis and 3 days after LPS exposure, respectively, concluded Samples 3 and 4.[26] The lung endothelial dataset was primarily used to explore the role of genes and changes in lung tissue. Rstudio software based on the R language was primarily used to analyze the transcriptome mixture. The Dplyr R package was used to handle complex data frames. Exclusion criteria for cells included less than 50 genes and too many mitochondrial genes (>7%). Subsequently, the Seruat package was used to normalize "LogNormalize." Seruat R package was also used to delete cells with low-quality sequencing. Preliminary downscaling for data mixture was also used to

discriminate and cluster cells based on characters, particularly gene expression situations.

### *Cell cluster identification and key pathway enrichment analysis*

First, "RunPCA" was used to identify the principal components of mixtures. Resolution was set to 0.9, and 20 integrating groups were obtained. Thereafter, irGSEA and Ucell packages were used to compute related pathway scores of every cell before drawing the heatmap based on the tSNE algorithm. Cell proportions developing pyroptosis based on gene expression levels were compared at different time points. We also described the trend for pyroptosis.

### *Transcriptomic analysis and weighted gene coexpression network analysis*

The GSE104214 dataset was downloaded to screen differentially expressed genes (DEGs). After preprocessing, the ssGSEA algorithm was performed to calculate the Pyroptosis and NOD scores for transcriptomic data. The DEGs between 24 h LPS and normal, and 24 h and 8 h LPS were analyzed using the limma package. A heatmap package was used to exhibit gene expression differences. The PN scores, LPS intervention time, and disease status were imported into the weighted correlation network analysis (WGCNA) to extract significant correlation genes with these features.

### *Spatial transcriptomics analysis and enrichment analysis*

The spatial transcriptomics dataset, GSE202322, was obtained from the GEO database. This dataset was about lungs from mice infected with the influenza A virus. R package Hksc was used to preprocess transcriptomics data and construct gene spatial distribution. The enrichment states of different spatial locations in the lungs were assessed by GSVA packages. Changes in the *Nlrp3* gene and pyroptosis were tracked along the timeline of the inflammation process.

### *Molecule docking analysis for targeting protein and ACT001*

The chemical structure file for ACT001 was downloaded from the PubChem database. Autodock 4.2 helped analyze the potential docking modes between protein and small drugs. Pymol software based on Python language was used to observe docking locations and generate chemical bonds or molecular forces.

### *Histopathological analysis*

Twenty-four hours after model establishment, mice were anesthetized and lung tissue was perfused via the right ventricle with 5 mL precooled PBS. Lung lobes were isolated and fixed in 4% paraformaldehyde for 48 h. Fixed lungs were embedded in paraffin, sectioned at 5 μm, and stained with hematoxylin–eosin (H&E). These sections were imaged (at least 6 randomly selected areas) and scored for lung injury scores by two independent investigators.[27]

### *Bronchoalveolar lavage fluid collection and cell counting*

Mice were anesthetized and tracheally intubated in a separate experiment. Alveolar lavage was collected by injecting 0.8 mL of precooled PBS into the lungs and repeated thrice. The collected BALF was centrifuged at 300 g in 4°C for 10 min. The supernatant was stored at −80°C for cytokine analysis. Cell aliquots were stained with Trypan Blue (Solarbio, Beijing, China). Total cells were determined using a hemacytometer.

### *Cell culture and the activation of NLRP3 inflammasome*

Bone marrow cells were isolated from femurs of 9–10-weeks-old C57BL/6 mice. The resulting cells were cultured in Iscove's Modified Dulbecco's medium (IMDM) containing 20% L929 cell supernatant, and 10% fetal bovine serum (Gibco, Grand Island, NY, USA), 1% penicillin, and streptomycin. On Day 3, 10 mL of fresh IMDM complete medium was added. On Day 7, BMDMs were harvested and seeded into a 24- or 12-well culture dishes for further experiments. All cells were cultured at 37°C in a constant temperature incubator (Thermo, Waltham, MA, USA) with 5% $CO_2$ humidity.

NLRP3 inflammasome activation was induced for 4 h priming with LPS (100 ng/mL, Sigma, USA) before challenging with NLRP3 activator ATP (5 mM, Sigma, USA) for 30 min. ACT001 (2.5 μM, 5 μM, or 10 μM) was added simultaneously with LPS. Before LPS treatment, Mdivi-1 (20 μM, Shanghai, China) was preincubated for 30 min.

### *Protein immunoblotting*

Whole lung tissue and cell lysates with a protease and a phosphatase inhibitor cocktail in RIPA buffer were prepared. Equal amounts of protein were separated by 8–12% SDS-PAGE. The separated protein bands were then transferred to a PVDF membrane. The membrane was blocked for 1 h with 5% BSA and then incubated with primary antibodies against DRP1 (ab184248, Abcam, USA), Mitofusin2 (ab56889, Abcam, USA), NLRP3 (ab263899, Abcam, USA), cleaved caspase-1 (89332s, CST, MA, USA), GSDMD (ab219800, Abcam, USA), ß-actin (4970S, CST, MA, USA) overnight at 4°C. The next day, PVDF membranes were incubated with secondary antibodies for 1 h, and the target bands were detected using an enhanced chemiluminescence (ECL) kit (Millipore, Billerica, MA, USA). ImageJ software was used for quantitative protein analysis.

### *ELISA*

IL-1ß and THF-α levels in BALF supernatants and cell culture media were measured using ELISA kits (R&D Systems,

USA). Specific procedures were strictly followed according to the manufacturer's instructions.

### *Propidium Iodide (PI)*

After the intervention, PI (Beyotime, Shanghai, China) was added to 24-well plates and placed in an incubator (Thermo, USA) at 37°C with 5% $CO_2$ for 15 min for staining. Cells (at least five fields per well) were then imaged under a fluorescence microscope (Olympus, Japan) at magnification 400X.

### *Mitochondrial quantity and morphology analysis*

After NLRP3 inflammasome activation, BMDMs were stained with Mito Tracker Red (50 nM, Thermo Fisher Scientific, Waltham, MA, USA) for 30 min. The cells were washed thrice with PBS and fixed with 4% formaldehyde for 30 min. Cells were rewashed with PBS thrice before analysis of cell images under fluorescence and confocal microscopes (FV1200, OLYMPUS). The ImageJ macro was used to quantify mitochondrial morphology, including mitochondrial interconnectivity (ratio of the mean area and the mean perimeter) and mitochondrial elongation (the inverse circularity). A total of 20 cells were measured in each group.

## Results

### *Pyroptosis and NOD pathway-related gene identification*

As shown in Figure 2A, seven genes representing pyroptosis and the NOD pathway were selected from two gene datasets with their biological functions. The PPI network (Figure 2B) was constructed using six proteins expressed by selected genes. In mRNA transcriptomics, pyroptosis enrichment was typically high after the effect of LPS and became highest during the first 24 h (Figure 2C). This was in line with the following single-cell analysis, indicating that pyroptosis rapidly occurs during pathogen invasion.

### *Single-cell PN degree evaluation*

In Figure 2D, the PN score was lower at the beginning of LPS influencing lung endothelial cells, at 6-h timepoint.

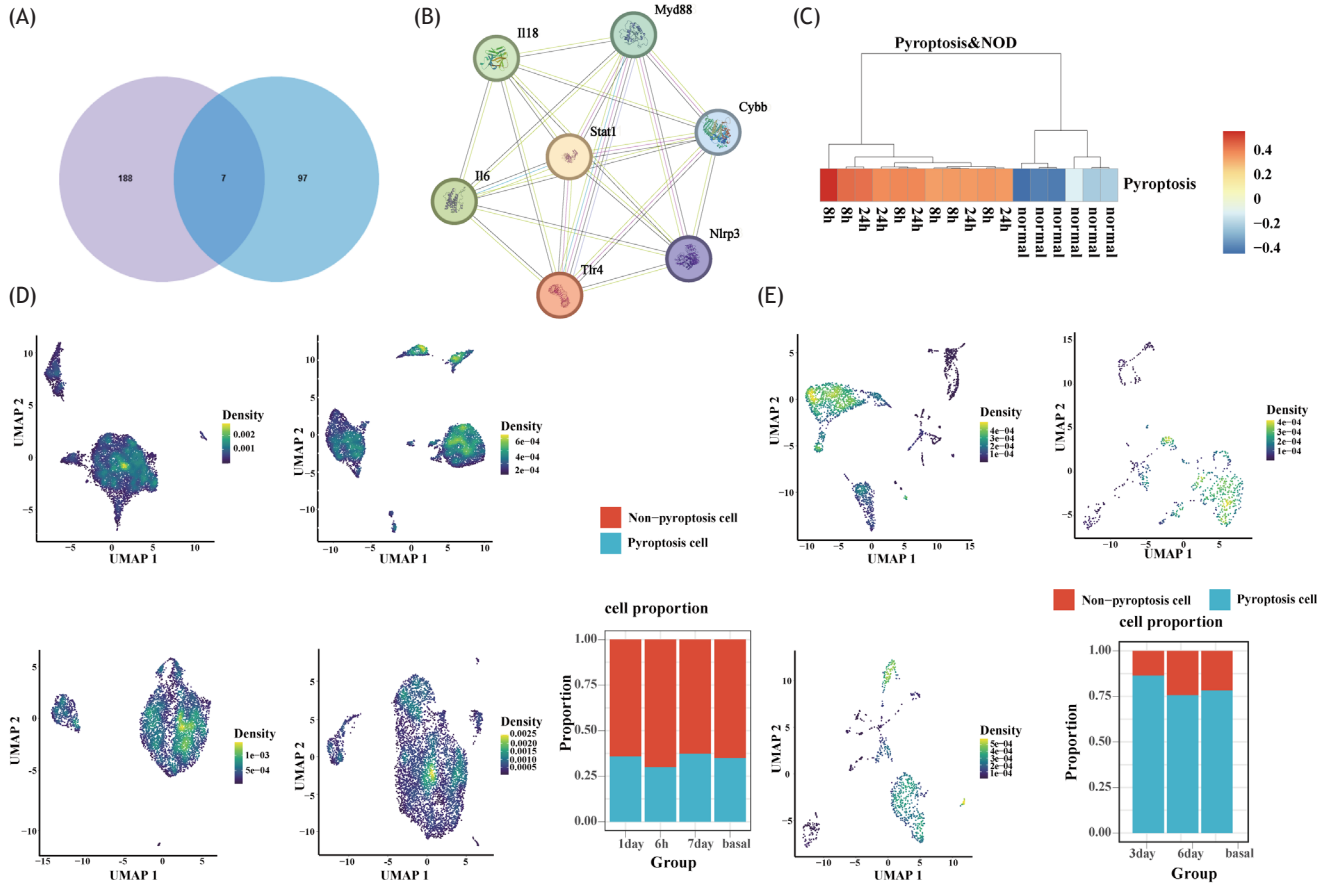


**Figure 2** NLRP3-dependent pyroptosis significantly correlated with acute lung injury (ALI). (A) Venn diagram of NOD pathway and pyroptosis-related gene markers; (B) PPI network of NOD and pyroptosis-related genes; (C) Scores of pyroptosis and NOD in RNA-seq dataset. Different colors represent scores, X-axis represents LPS interfering times; (D) Trend and changes of PN in endothelial cell single cell level after LPS; (E) Trend and changes of PN in resident macrophage at single cell level after LPS.

However, the PN score became higher than the basal situation after 24 h, suggesting the gradual occurrence of pyroptosis. At 7 days, the score was the highest, suggesting the occurrence of cell death. These results indicate that pyroptosis influenced the whole process during LPS intervention.

For macrophages, assembled results were found. Influenced by LPS, ALI arose, accompanied by an increase in PN high-expressing cells (Figure 2E).

### *Identification of differentially expressed genes and pyrotposis-related genes*

In Figure 3A, we screened 2156 and 2398 mRNAs as DEGs. Following WGCNA analysis was surrounding these genes. In WGCNA analysis (Figure 3B), the turquoise module highly correlated with pyroptosis and inflammation development times was identified. In this module gene set, Nlrp3 overlapped with NOD pathway and pyroptosis genes. Therefore, Nlrp3 was specifically identified as a hub biomarker for our study.

### *Spatial time distribution of Nlrp3 and pyroptosis*

In Figure 3C, three timepoints were recorded, that is, 0, 3, and 9 days. For the Nlrp3 gene, we observed an increasing number of high-expression dots, representing cell clusters. This indicates that a significant portion of lung tissue had high spatial Nlrp3 expression. Pyroptosis enrichment was also tracked (Figure 3D). The trend was positive, a larger region exhibited pyroptosis phenomena with the inflammation increasing by virus invasion.

### *Molecular docking*

In the most reliable mode, the free binding energy was −5.74 kcal/mol, less than −5, suggesting a reliable conjunction between small molecular drugs and NLRP3 protein. Figure 3E shows several polar and nonpolar interaction constructions.

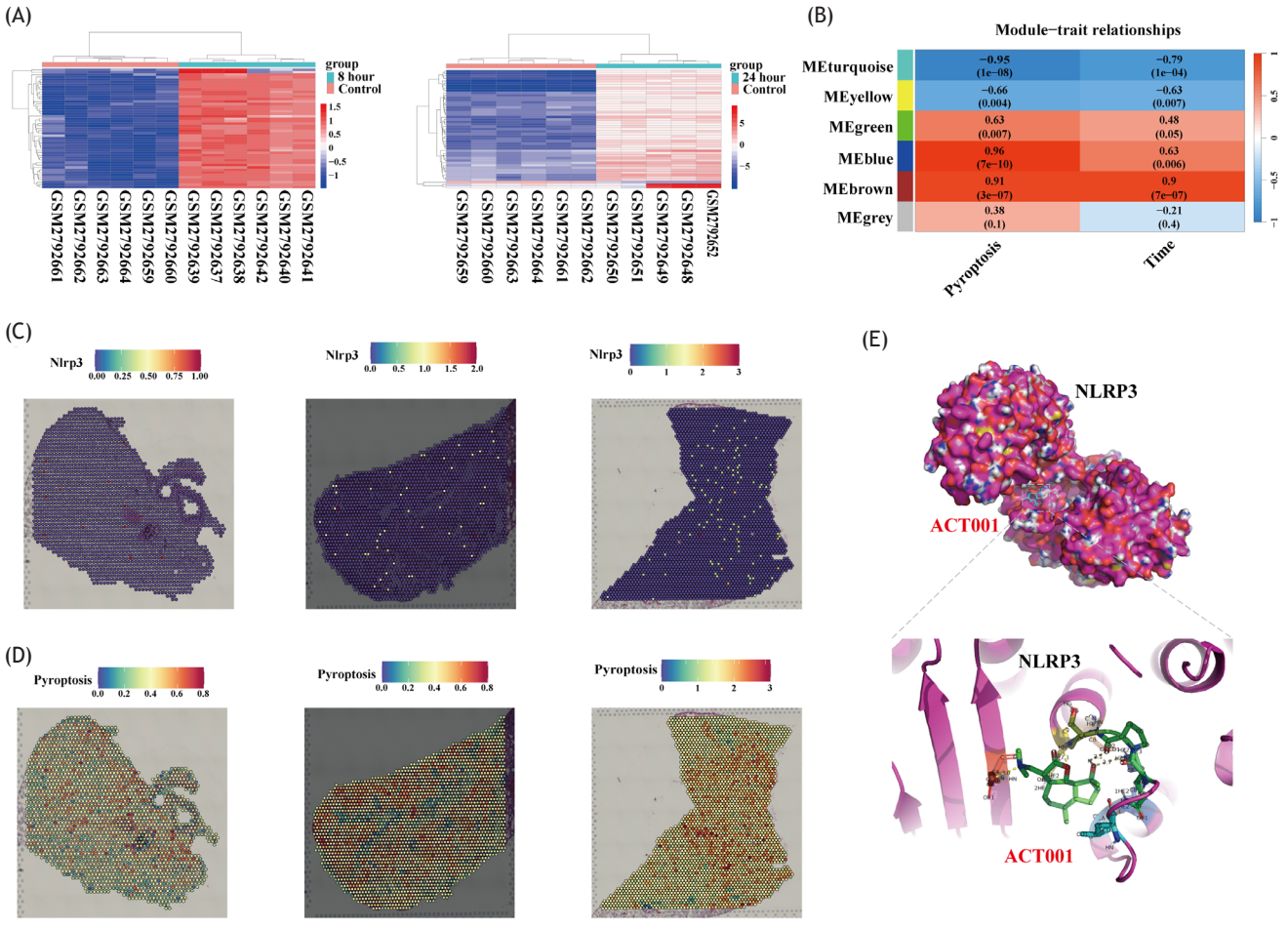


**Figure 3** NLRP3 is strongly associated with ALI severity and molecular docking of ACT001 and NLRP3. (A) Heatmap of top 50 DEGs after LPS. Three groups, 8 h, 24 h, and control were compared; (B) WGCNA module correlation heatmap in RNA-seq. Different colors represent the degree of correlation; (C) The landscape of NLRP3 spatial distribution in 3 time points; (D) The landscape of pyroptosis gene enrichment spatial distribution in 3 time points; (E) Molecular docking diagram of NLRP3 and ACT001. Lines marked with yellow represent intermolecular force.

### *ACT001 inhibits LPS-induced acute lung injury*

The NLRP3 inflammasome also instigates ALI in which the lung parenchyma and resident immune cells generate IL-1β and IL-18 to drive pulmonary inflammation.[28,29] The in vivo therapeutic efficacy of ACT001 was evaluated in a well-established mouse model of LPS-induced ALI. As shown in Figure 4A–C, histological assessment of lung sections revealed that ACT001 prevented alveolar neutrophils, interstitial neutrophils, hyaline membranes, proteinaceous debris, and alveolar septal thickening in a dose-dependent manner. Although significant body weight loss was observed in the LPS-injected group, the mice treated with the ACT001 recovered (Figure 4D). In Figure 4E, only 10% of mice receiving LPS via intratracheal (i.t.) administration (20 mg/kg) survived beyond 7 days. In contrast, a single injection of either ACT001 (100 mg/kg) or ACT001 (200 mg/kg) 2 h before LPS administration rescued 50 or 60% of the mice. Besides, therapeutic ACT001 inhibited protein concentration and total number of cells, and decreased IL-1β in BALF in a dose-dependent manner. Meanwhile, ACT001 downregulated *Nlrp3* mRNA transcript more significantly with increasing concentration (Figure 4F–I). Consistently, ACT001 limited NLRP3 inflammasome activation and reduced mortality of mice challenged with LPS.

### *ACT001 inhibits NLRP3 inflammasome activity in a dose-dependent manner in vitro*

To probe the sensitivity of BMDMs to ACT001, BMDMs were exposed to various concentrations of ACT001 (0, 7.81, 15.63, 31.25, 62.5, 125, 250, 500, and 1000 μM) for 24 h. Figure 5A shows that the IC50 value of the BMDMs for ACT001 was 17.43 μM. This value provides a safe range and guides the treatment concentration for subsequent experiments. The molecular docking results in Figure 3E showed that ACT001 binds to NLRP3. Therefore, LPS plus ATP stimulation was administered to stimulate NLRP3 inflammasome activation in BMDMs. ACT001 downregulated NLRP3 expression, cleaved-caspase-1, and GSDMD-cleaved in a dose-dependent manner, which indicated a reduction

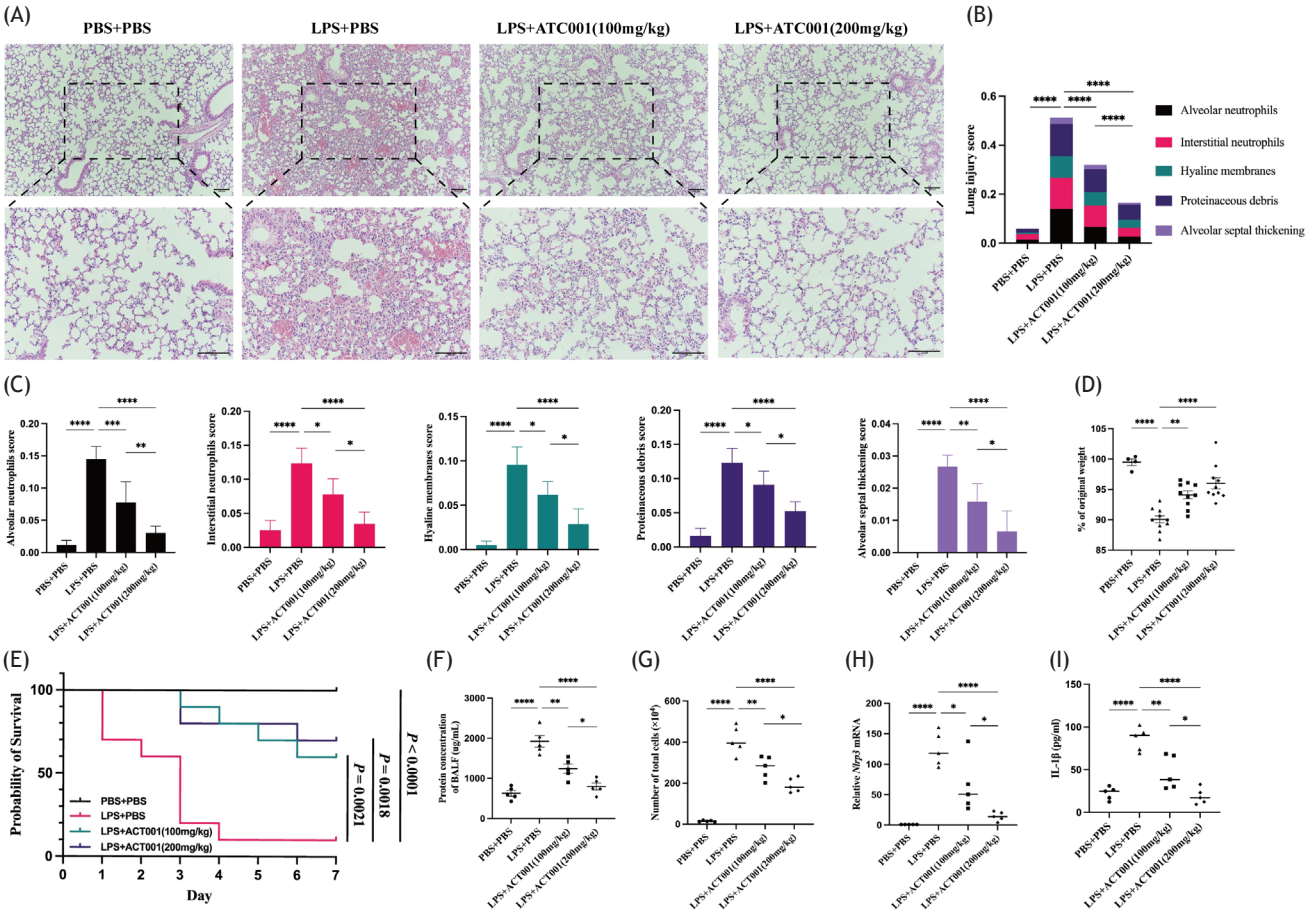


**Figure 4** ACT001 inhibits LPS-induced acute lung injury. (A) The histopathological changes of mouse lung sections (n = 5 per group; scale bar = 100 μm); (B) Weighted total lung injury score based on 5 pathological features score; (C) Alveolar neutrophils score, interstitial neutrophils score, hyaline membranes score, proteinaceous debris score, and alveolar septal thickening score of 5 pathological features score; (D) Changes in body weight of mice; (E) Survival analysis of the mice (n = 10 per group); The protein concentration (F) and total number of cells (G) in BALF; H) The *Nlrp3* mRNA level of the lung tissue; I) The IL-1β level in the BALF. Data were presented as mean ± SD (*P < 0.05; **P < 0.01; ***P < 0.001; ****P < 0.0001).

in the NLRP3 inflammasome activation (Figure 5B). Although the level of IL-1β in the supernatants decreased with increasing doses of ACT001, no significant change was observed in the TNF-α levels (Figure 5C). Moreover, ACT001 repressed Nlrp3, caspase-1, IL-1β, and IL-18 at the transcriptional level (Figure 5D). Taken together, these data indicate that ACT001 inhibits NLRP3 inflammasome activation in a dose-dependent manner in vitro.

### *ACT001 inhibits the activity of NLRP3 inflammasome by DRP1*

The exposure of macrophages to NLRP3 activators causes mitochondrial damage.[30] We wondered whether the anti-inflammatory effects of ACT001 are mitochondrially exerted and blunted NLRP3 inflammasome activation. Consequently, we observed significant damage in the mitochondrial network, including mitochondrial interconnectivity and elongation in the LPS plus ATP group (Figure 6A,B). Notably, the ACT001 treatment showed a protective effect on the reticular integrity of mitochondria (Figure 6A,B). Meanwhile, ACT001 showed an inhibitory effect on the mitochondrial fission protein DRP1, whereas no significant effect was observed on the mitochondrial fusion protein Mitofusin2 (Figure 6C). The Mdivi-1, an inhibitor of DRP1, was used to dissect the roles of DRP1 for NLRP3 inflammasome activation. As shown in Figure 6D,E, Mdivi-1 treatment reduced NLRP3-dependent pyroptosis, induced by LPS plus ATP stimulation. ACT001 treatment showed pyroptosis inhibition similar to that of Mdivi-1. Furthermore, both ACT001 and Mdivi-1 suppressed IL-1β secretion following NLRP3 inflammasome activation.

## Discussion

This study integrated the analyzed transcriptomics on single cell and spatial for the role of pyroptosis mechanisms involved in acute lung injury. Considering the

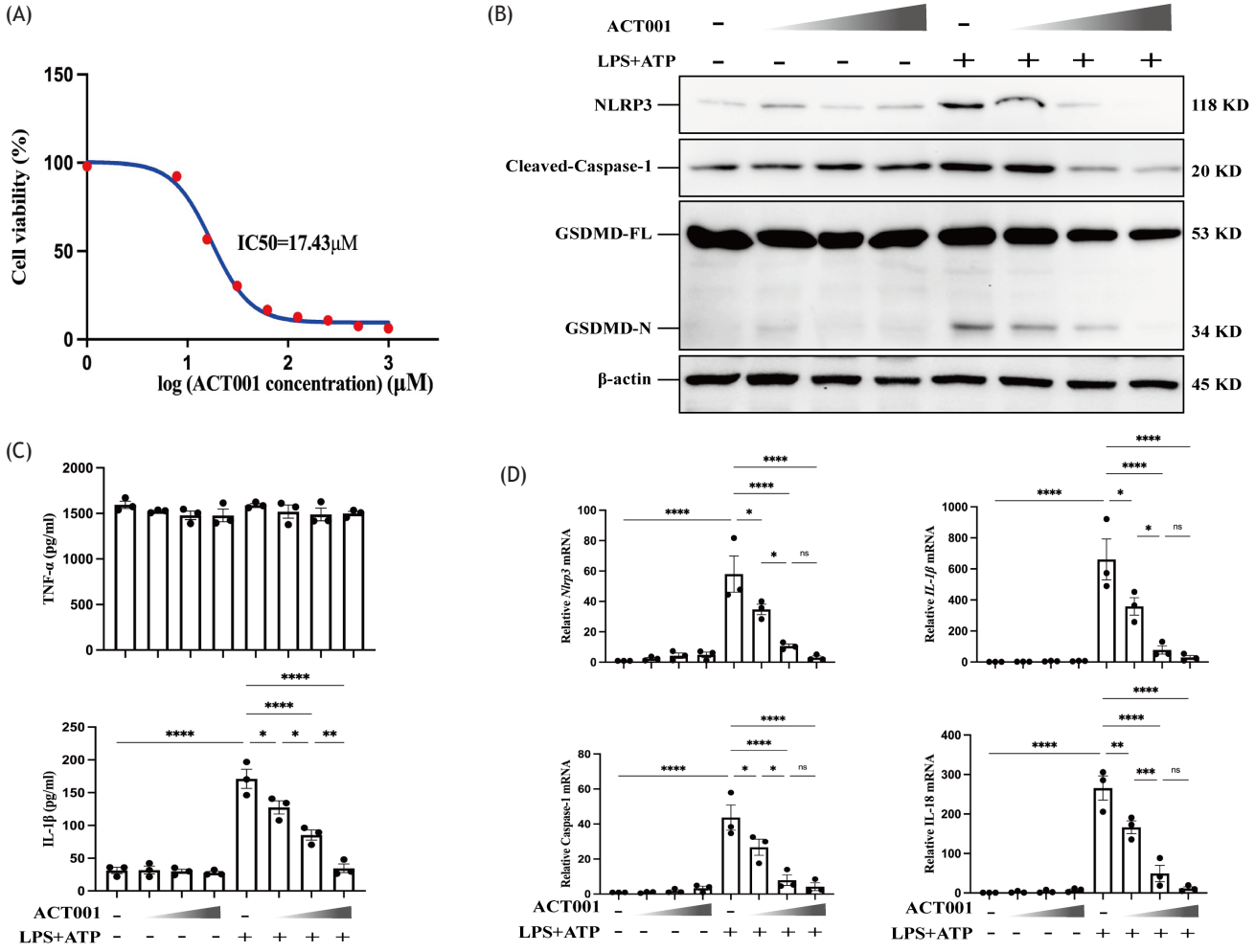


**Figure 5** ACT001 inhibits the activity of NLRP3 inflammasome in a dose-dependent manner in vitro. (A) The IC50 of BMDM was treated with various concentrations of ACT001; (B–D) BMDMs were exposed to LPS (100 ng/mL) with or without ACT001 (2.5 uM, 5 uM, or 10 uM) for 4 h before adding ATP (5 mM) for 30 min. Immunoblotting results (B) of the NLRP3, cleaved caspase-1, GSDMD (FL and N); (C) The TNF-α and IL-1β levels in the supernatants; (D) The mRNA expression levels of *Nlrp3*, *caspase-1*, *IL-1β*, and *IL-18* were assayed from the BMDMs (n = 3). Data were presented as mean ± SD (*P < 0.05; **P < 0.01; ***P < 0.001; ****P < 0.0001).

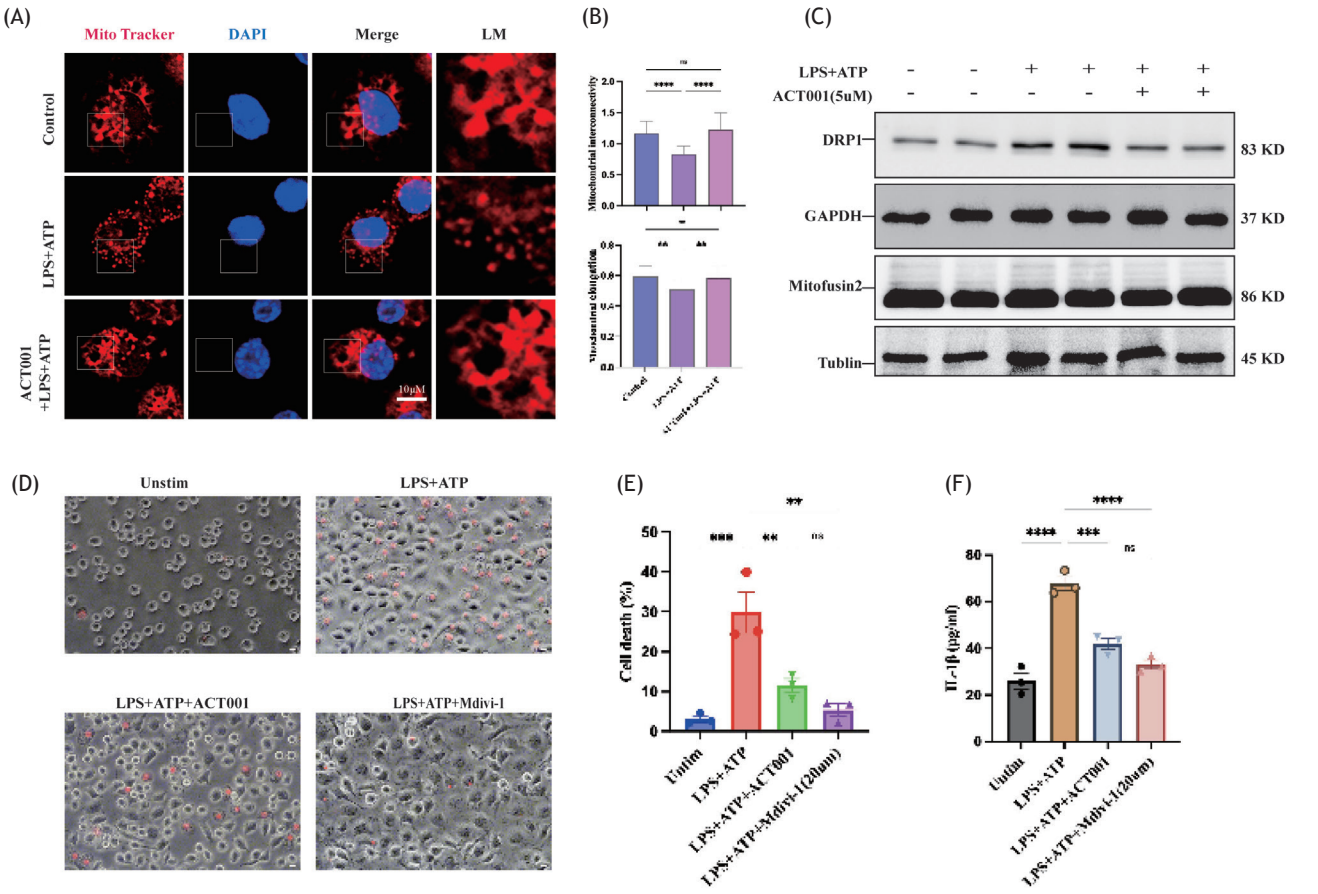


**Figure 6** ACT001 inhibits the activity of NLRP3 inflammasome by DRP1. (A) Confocal microscopic images of BMDMs were exposed to LPS (100 ng/mL) with or without ACT001 (5 uM) for 4 h before adding ATP (5 mM) for 30 min. The mitochondrial network was stained by Mito Tracker; the scale bar represents 10 μm; (B) Mitochondrial interconnectivity (ratio of the mean area and the mean perimeter) and elongation (the inverse circularity) were quantified by ImageJ macro (n = 20 cells); (C) Immunoblot results of DRP1 and Mitofusin2 when treated ACT001 with or without LPS plus ATP (n = 3); (D and E) PI images and quantification; (F) The IL-1β levels in the supernatants (n = 3). Data were presented as mean ± SD (*P < 0.05; **P < 0.01; ***P < 0.001; ****P < 0.0001).

theoretical basis, we further explored the effects of ACT001. Consequently, ACT001 protected the lungs against pyroptosis both in vivo and in vitro.

In mRNA transcriptomics and single analysis, pyroptosis represented a strong relationship with inflammation phases in the entire lung microenvironment. As a unique form of cell death, activation of NLRP3 inflammasome could result in significant pathogen invasion.[31] The effects of pyroptosis were also distinguished at different stages. Pyroptosis during its early stages primarily aided in clearing abnormal or damaged cells, activating replicating pathogens, and protecting vulnerable organs. Pyroptosis would interfere with normal cell status and physical functions accompanied by secretion of inflammation factors.[4] Many studies have reported the phenomena and molecular correlation between NOD-receptor-like pathways and pyroptosis.[32] Sepsis or inflammation, and NLRP3 have also been found to mediate pyroptosis.[33,34] For lung endothelial cells, the enrichment of pyroptosis genes in this study rapidly increased at the first 6 h after CLP operation, representing positive effects during this period. After the acute phase, however, the enrichment increased after decreasing in the early inflammation stage, indicating remarkable cell death. Gene expression was consistent with that reported in previous studies. Endothelial cells, immune cells, and resident macrophages in the lungs were also found to be of assembled trends of pyroptosis enrichment. mRNAs also explained the roles of pyroptosis mechanisms. mRNA transcriptomics was used to identify potential disease biomarkers possessing time and pyroptosis dependency. Interestingly, the Nlrp3 gene was screened and as a pyroptosis marker gene, it was a diagnostic biomarker with close relationships with whole pyroptosis and sepsis development.

We first measured certain markers in vivo for validation. Previous studies on pyroptosis in lung injury focused on alveolar macrophages.[35] Our study first confirmed that lung injury can be treated by ACT001. Gene expression change of Nlrp3 was blocked, which was consistent with our bioinformatics analysis. Evidence for the protective effects of ACT001 in mRNA and tissue level was validated.

Some investigations have reported in vivo biological safety and metabolisms of ACT001; its lack of accumulation and rapid distribution in vivo ensures its potential application as medication.[18] In this regard, our study examined

the IC50 of BMDMs, one of the most important immune cell species in the lungs to establish a broad safe range. The measured IC50 (17.43 μM) indicated mild cytotoxicity. Macrophages were thought to aggravate other types of lung injury, such as lung ischemic reperfusion; IL-1R/NF-κB/NLRP3 pathway was also involved.[36] Thus, the proposed hypothesis indicates that ideal drugs ought to decrease caspase-1 and IL-1β secretion, promoting inflammation and cell deaths surrounding the macrophages. Herein, we observed downregulation of caspase-1, GSDMD, and Nlrp3 under different ACT001 concentrations. In contrast to ACT001, double-stimulating operations (LPS + ATP) increased the protein levels of these markers. The inversion phenomena demonstrated that ACT001 can decrease the generation of pyroptosis inducers and abnormal monocytes.

We observed abnormal changes in mitochondrial interconnectivity and elongation in cell environments imitating sepsis. Meanwhile, cell death markers were also highly expressed. These indicate that mitochondrial changes are accompanied by pyroptosis occurrence. ALI is often caused by NLRP3 inflammasome activation and mitochondrial abnormal changes simultaneously.[37] Our findings revealed that ACT001 depressed the two cell death engines. The observed protection effects included mitochondrial indicators, interconnectivity and elongation, mitochondrial quality marker protein, DRP1, and Mitofusion2. The role of mitochondria was also preserved.

This study has some limitations. First, the dynamic intracellular progress of ACT001 was not observed, and the subcellular location was inadequate. Additionally, we did not investigate more precise regulation mechanisms between ACT001 and pyroptosis, a subject of further research. Third, these limitations hinder the clear observation of these relationships, and require an exploration of the noncoding RNAs involved.

In conclusion, depending on integrative transcriptomics analysis, we demonstrated that Nlrp3 gene activation and pyroptosis are closely associated with ALI development. In vivo experiments validated these bioinformatic analysis and protection effects of ACT001 on the lungs. NLRP3 activation and pyroptosis were suppressed in vitro after treatment with ACT001. Furthermore, mitochondrial fusion and fission disorders induced by excess ROS production were prevented due to ACT001 in macrophages.

## Conclusions

Our study revealed that pyroptosis-related genes were highly expressed in single-cell and spatial mapping along the first week of ALI occurrence. Meanwhile, ACT001 significantly reduced pyroptosis in ALI through the DRP1/NLRP3 pathway.

## Conflict of Interests

The authors have declared that no conflicts of interest exist. We acknowledge that no AI has been applied to this paper.

## Authors' contributions

Yan Fan contributed to the data analysis, investigation, visualization, and writing of the original draft. Yuanlin Wang was involved in the formal analysis, software, visualization, and writing, review, and editing of the manuscript. Weiwei Zhang contributed to the investigation and methodology. Keliang Xie contributed to the project administration, conceptualization, writing review, and funding acquisition.

## Financial support and sponsorship

Not applicable to this study.

## Declaration of competing interest

The authors declare no known competing financial interests or personal relationships.

## Ethics declaration

This study was approved by the Ethics Committee of Tianjin Medical University (IRB2022-DWFL-587).

## References

1. Lin M, Stewart MT, Zefi S, Mateti KV, Gauthier A, Sharma B, et al. Dual effects of supplemental oxygen on pulmonary infection, inflammatory lung injury, and neuromodulation in aging and COVID-19. Free Radic Biol Med. 2022;190:247–63. https://doi.org/10.1016/j.freeradbiomed.2022.08.004
2. Sadowitz B, Roy S, Gatto LA, Habashi N, Nieman G. Lung injury induced by sepsis: Lessons learned from large animal models and future directions for treatment. Expert Rev Anti Infect Ther. 2011;9(12):1169–78. https://doi.org/10.1586/eri.11.141
3. Zhang LY, Zhang JG, Yang X, Cai MH, Zhang CW, Hu ZM. Targeting tumor immunosuppressive microenvironment for the prevention of hepatic cancer: Applications of traditional Chinese medicines in targeted delivery. Curr Top Med Chem. 2020;20(30):2789–800. https://doi.org/10.2174/1568026620666201019111524
4. Gao YL, Zhai JH, Chai YF. Recent advances in the molecular mechanisms underlying pyroptosis in sepsis. Mediat Inflamm. 2018;2018:5823823. https://doi.org/10.1155/2018/5823823
5. Yang M, Yang X, Wang S, Xu L, Ke S, Ding X,et al. HMGB1-induced endothelial cell pyroptosis is involved in systemic inflammatory response syndrome following radiofrequency ablation of hepatic hemangiomas. Am J Transl Res. 2019;11(12):7555–67.
6. Ross C, Chan AH, von Pein JB, Maddugoda MP, Boucher D, Schroder K. Inflammatory caspases: Toward a unified model for caspase by inflammasomes. Annu Rev Immunol. 2022;40:249–69. https://doi.org/10.1146/annurev-immunol-101220-030653
7. Andreeva L, David L, Rawson S, Shen C, Pasricha T, Pelegrin P, et al. NLRP3 cages revealed by full-length mouse NLRP3 structure control pathway activation. Cell. 2021;184(26):6299–6312.e22. https://doi.org/10.1016/j.cell.2021.11.011
8. Xian H, Watari K, Sanchez-Lopez E, Offenberger J, Onyuru J, Sampath H, et al. Oxidized DNA fragments exit mitochondria via mPTP- and VDAC-dependent channels to activate

NLRP3 inflammasome and interferon signaling. Immunity. 2022;55(8):1370–1385.e8. https://doi.org/10.1016/j.immuni.2022.06.007
9. Lamkanfi M, Dixit VM. Inflammasomes and their roles in health and disease. Annu Rev Cell Dev Biol. 2012;28:137–61. https://doi.org/10.1146/annurev-cellbio-101011-155745
10. Rao A, Barkley D, França GS, Yanai I. Exploring tissue architecture using spatial transcriptomics. Nature. 2021;596(7871):211–20. https://doi.org/10.1038/s41586-021-03634-9
11. Stuart T, Satija R. Integrative single-cell analysis. Nature Rev Genet. 2019;20(5):257–72. https://doi.org/10.1038/s41576-019-0093-7
12. Toya SP, Li F, Bonini MG, Gomez I, Mao M, Bachmaier KW, et al. Interaction of a specific population of human embryonic stem cell-derived progenitor cells with CD11b+ cells ameliorates sepsis-induced lung inflammatory injury. Am J Pathol. 2011;178(1):313–24. https://doi.org/10.1016/j.ajpath.2010.09.041
13. Wang F, Chen M, Ma J, Wang C, Wang J, Xia H, et al. Integrating bulk and single-cell sequencing reveals the phenotype-associated cell subpopulations in sepsis-induced acute lung injury. Front Immunol. 2022;13:981784. https://doi.org/10.3389/fimmu.2022.981784
14. Pita-Juarez Y, Karagkouni D, Kalavros N, Melms JC, Niezen S, Delorey TM, et al. A single-nucleus and spatial transcriptomic atlas of the COVID-19 liver reveals topological, functional, and regenerative organ disruption in patients. BioRxiv [Preprint]. 2022:2022. https://doi.org/10.1101/2022.10.27.514070
15. Freund RRA, Gobrecht P, Fischer D, Arndt HD. Advances in chemistry and bioactivity of parthenolide. Nat Prod Rep. 2020;37(4):541–65. https://doi.org/10.1039/c9np00049f
16. Pareek A, Suthar M, Rathore GS, Bansal V. Feverfew (*Tanacetum parthenium* L.): A systematic review. Pharmacogn Rev. 2011;5(9):103–10. https://doi.org/10.4103/0973-7847.79105
17. Jin P, Madieh S, Augsburger LL. The solution and solid state stability and excipient compatibility of parthenolide in feverfew. AAPS PharmSciTech. 2007;8(4):E105. https://doi.org/10.1208/pt0804105
18. Xi XN, Liu N, Wang QQ, Wu HT, He HB, Wang LL, et al. Pharmacokinetics, tissue distribution and excretion of ACT001 in Sprague-Dawley rats and metabolism of ACT001. J Chromatogr B Analyt Technol Biomed Life Sci. 2019;1104:29–39. https://doi.org/10.1016/j.jchromb.2018.11.004
19. Guo H, Song Y, Li F, Fan Y, Li Y, Zhang C, et al. ACT001 suppressing M1 polarization against inflammation via NF-kappaB and STAT1 signaling pathways alleviates acute lung injury in mice. Int Immunopharmacol. 2022;110:108944. https://doi.org/10.1016/j.intimp.2022.108944
20. Li J, Li SS, Guo JS, Li Q, Long J, Ma C, et al. Natural product micheliolide (MCL) irreversibly activates pyruvate kinase M2 and suppresses leukemia. J Med Chem. 2018;61(9):4155–64. https://doi.org/10.1021/acs.jmedchem.8b00241
21. Bahrami M, Kamalinejad M, Latifi SA, Seif F, Dadmehr M. Cytokine storm in COVID-19 and parthenolide: Preclinical evidence. Phytother Res. 2020;34(10):2429–30. https://doi.org/10.1002/ptr.6776
22. Gadepalli VS, Kim H, Liu Y, Han T, Cheng L. XDeathDB: A visualization platform for cell death molecular interactions. Cell Death Dis. 2021;12(12):1156. https://doi.org/10.1038/s41419-021-04397-x
23. Chen T, Zhang H, Liu Y, Liu YX, Huang L. EVenn: Easy to create repeatable and editable Venn diagrams and Venn networks online. J Genet Genomics. 2021;48(9):863–6. https://doi.org/10.1016/j.jgg.2021.07.007
24. Szklarczyk D, Gable AL, Nastou KC, Lyon D, Kirsch R, Pyysalo S, et al. The STRING database in 2021: Customizable protein-protein networks, and functional characterization of user-uploaded gene/measurement sets. Nucleic Acids Res. 2021;49(D1):D605–D612. https://doi.org/10.1093/nar/gkaa1074
25. Armand EJ, Li J, Xie F, Luo C, Mukamel EA. Single-cell sequencing of brain cell transcriptomes and epigenomes. Neuron. 2021;109(1):11–26. https://doi.org/10.1016/j.neuron.2020.12.010
26. Moore PK, Anderson KC, McManus SA, Tu TH, King EM, Mould KJ, et al. Single-cell RNA sequencing reveals unique monocyte-derived interstitial macrophage subsets during lipopolysaccharide-induced acute lung inflammation. Am J Physiol Lung Cellular Mol Physiol. 2023;324(4):L536–L549. https://doi.org/10.1152/ajplung.00223.2022
27. Matute-Bello G, Downey G, Moore BB, Groshong SD, Matthay MA, Slutsky AS, et al. An official American Thoracic Society workshop report: Features and measurements of experimental acute lung injury in animals. Am J Respir Cell Mol Biol. 2011;44(5):725–38. https://doi.org/10.1165/rcmb.2009-0210ST
28. Grailer JJ, Canning BA, Kalbitz M, Haggadone MD, Dhond RM, Andjelkovic AV, et al. Critical role for the NLRP3 inflammasome during acute lung injury. J Immunol. 2014;192(12):5974–83. https://doi.org/10.4049/jimmunol.1400368
29. Xian H, Liu Y, Rundberg Nilsson A, Gatchalian R, Crother TR, Tourtellotte WG, et al. Metformin inhibition of mitochondrial ATP and DNA synthesis abrogates NLRP3 inflammasome activation and pulmonary inflammation. Immunity. 2021;54(7):1463–77 e11. https://doi.org/10.1016/j.immuni.2021.05.004
30. Zhong Z, Liang S, Sanchez-Lopez E, He F, Shalapour S, Lin XJ, et al. New mitochondrial DNA synthesis enables NLRP3 inflammasome activation. Nature. 2018;560(7717):198–203. https://doi.org/10.1038/s41586-018-0372-z
31. Bedoui S, Herold MJ, Strasser A. Emerging connectivity of programmed cell death pathways and its physiological implications. Nat Rev Mol Cell Biol. 2020;21(11):678–95. https://doi.org/10.1038/s41580-020-0270-8
32. Shao Y, Jiang Y, Wang J, Li H, Li C, Zhang D. Inhibition of circulating exosomes release with GW4869 mitigates severe acute pancreatitis-stimulated intestinal barrier damage through suppressing NLRP3 inflammasome-mediated pyroptosis. Int Immunopharmacol. 2023;126:111301. https://doi.org/10.1016/j.intimp.2023.111301
33. Liu L, Zhou L, Wang L, Mao Z, Zheng P, Zhang F, et al. MUC1 attenuates neutrophilic airway inflammation in asthma by reducing NLRP3 inflammasome-mediated pyroptosis through the inhibition of the TLR4/MyD88/NF-κB pathway. Respir Res. 2023;24(1):255. https://doi.org/10.1186/s12931-023-02550-y
34. Huang Y, Lin J, Wu Z, Li Y. Circular RNA circVAPA modulates macrophage pyroptosis in sepsis-induced acute lung injury through targeting miR-212-3p/Sirt1/Nrf2/NLRP3 axis. Int J Exp Pathol. 2024;105(1):21–32. https://doi.org/10.1111/iep.12497
35. Fu Q, Shen N, Fang T, Zhang H, Di Y, Liu X, et al. ACT001 alleviates inflammation and pyroptosis through the PPAR-γ/NF-κB signaling pathway in LPS-induced alveolar macrophages. Genes Genomics. 2024;46(3):323–32. https://doi.org/10.1007/s13258-023-01455-w
36. Zhou P, Guo H, Li Y, Liu Q, Qiao X, Lu Y, et al. Monocytes promote pyroptosis of endothelial cells during lung ischemia-reperfusion via IL-1R/NF-κB/NLRP3 signaling. Life Sci. 2021;276:119402. https://doi.org/10.1016/j.lfs.2021.119402
37. White A, Wang Z, Wang X, King M, Guo C, Mantsounga C, et al. NLRP3 inflammasome activation in cigarette smoke priming for *Pseudomonas aeruginosa*-induced acute lung injury. Redox Biol. 2022;57:102467. https://doi.org/10.1016/j.redox.2022.102467